

# Study of Nd<sup>3+</sup> ion as a Dopant in YAG and Glass Laser

Kireet Semwal<sup>1\*</sup>, S. C. Bhatt<sup>2</sup>

<sup>1</sup>Department of Physics, G.B. Pant Engineering College, Pauri (Garhwal), India

<sup>2</sup>Department of Physics, HNB Garhwal Centrel University, Srinagar (Garhwal), India

\*Corresponding author: kireetsemwal@hotmail.com

Received December 31, 2012; Revised March 05, 2013; Accepted March 10, 2013

**Abstract** Trivalent neodymium (Nd<sup>3+</sup>) is the most successful type of active ion for solid-state lasers and thus far has been made to lase in more types of crystal and glass hosts than any other ion. It can operate as either a pulsed or continuous-wave laser with a sharp emission line. The most common emission wavelength is near 1 $\mu$ m, but there are several possible laser transitions in the near-infrared spectral region, and in addition a near-ultraviolet laser line. Although the effects of different host environments on the spectroscopic properties of Nd<sup>3+</sup> are more subtle than those for transition-metal ions, they can cause significant differences in lasing characteristics through changes in physical processes such as radiative transition strength, radiationless decay probabilities, excited-state absorption, and cross relaxation quenching. The Nd ion when doped into a solid-state host crystal produces the strongest emission at a wavelength just beyond 1 $\mu$ m. The two host materials most commonly used for this laser ion are yttrium aluminium garnet (YAG) and glass. At room temperature the 1.064 $\mu$ m radiative transition is homogeneous broadened with a narrow emission line width of 0.45nm and the upper level lifetime is 230 $\mu$ s. Nd can be doped to very high concentration in glass. The outstanding practical advantage compared to crystalline materials is the tremendous size capability for high-energy applications. The fluorescent lifetime is approximately 300 $\mu$ s, and, the emission line width is 18-28nm.

**Keywords:** Nd<sup>3+</sup>, Nd:YAG laser, Nd:Glass laser

## 1. Introduction

Materials for laser operation must possess sharp fluorescent lines, strong absorption bands, and reasonably high quantum efficiency for the fluorescent transition of interest. These characteristics are generally shown by solids (crystals or glass) which incorporate in small amount of elements in which optical transitions can occur between states of inner, incomplete electron shells. Thus the transition metals, the rare earth (lanthanide) series, and the actinide series are of interest in this connection. It is possible to co-dope many of these elements within solid-state host, chosen to obtain the desired long lifetime as well as other suitable laser properties. The sharp fluorescent lines in the spectra of crystals doped with these elements result from the fact that the outer shells from the surrounding crystal lattice shield the elements involved in transitions in the optical regime [4]. The host material must possess good optical properties as well good mechanical and thermal properties. Poor optical properties include variations in index of refraction, which lead to irregular beam quality in the laser output and impurities, which lead to scattering and undesired absorption of pump light or laser beam output. Poor mechanical and thermal properties lead to material deformation or fracturing of the host when the laser is operated under such high pulse-repetition rate or high steady state pumping. The host must also be able to accept the dopant material in a way that will not distort the desired properties of the dopant i.e.

a long lifetime and an appropriate line shape. The host must also be capable of being grown in size, with a uniform distribution of the dopant that is required for laser gain media [5].

The rare earth ions are natural candidates to serve as active ions in solid-state laser materials because they exhibit a wealth of sharp fluorescent transitions representing almost every region of the visible and near-infrared portions of the electromagnetic spectrum. It is a characteristic of these lines that they may be very sharp, even in the presence of the strong local fields of crystals, as a result of the shielding effect of the outer electrons. The outermost electrons of these ions form a complete rare gas shell, which is the xenon shell with two 5s and six 5p electrons. This shell is optically inactive. Next inside the xenon shell is the 4f shell, which is filled successively in passing from one element to the next. Trivalent cerium, Ce<sup>3+</sup>, has one 4f electron, and trivalent ytterbium, Yb<sup>3+</sup>, has 13. As long as the 4f shell is not completely filled with 14 electrons, a number 4f levels are unoccupied, and electrons already present in the 4f shell can be raised by light absorption into these empty levels. The sharp lines observed in rare earth absorption and emission spectra are ascribed to these transitions, and the sharpness of the lines is explained by the fact that the electrons making the transition lie inside the xenon shell and thus interact only weakly with outside ions. Table 1 shows the population of the outermost electron shells of the rare earths [4]. Rare earth ions usually exist in solids in either the trivalent or the divalent state. A divalent rare earth ion is formed when the atom gives up its outermost 6s electrons. When a

trivalent ion is formed the atom also loses its  $5d$  electron if it has one; otherwise, one of the  $4f$  electrons is lost. The rare earth ions generally have a number of sharp emission lines due to the atomic like character of the radiating  $4f$

state. They usually exist in solids in the trivalent form. Rare earth triple ions include neodymium ( $\text{Nd}^{3+}$ ), erbium ( $\text{Er}^{3+}$ ), holmium ( $\text{Ho}^{3+}$ ) and thulium ( $\text{Tm}^{3+}$ ) etc.

**Table 1. Electronic structure of elements 59 to 71**

| Number | Element      |    | Outermost electron shell |           |        |        |      |        |
|--------|--------------|----|--------------------------|-----------|--------|--------|------|--------|
| 54     | Xenon        | Xe | $4d^{10}$                | --        | $5s^2$ | $5p^6$ | --   | --     |
| 59     | Praseodymium | Pr | $4d^{10}$                | $4f^3$    | $5s^2$ | $5p^6$ | --   | $6s^2$ |
| 60     | Neodymium    | Nd | $4d^{10}$                | $4f^4$    | $5s^2$ | $5p^6$ | --   | $6s^2$ |
| 61     | Promethium   | Pm | $4d^{10}$                | $4f^6$    | $5s^2$ | $5p^6$ | --   | $6s^2$ |
| 62     | Samarium     | Sm | $4d^{10}$                | $4f^6$    | $5s^2$ | $5p^6$ | --   | $6s^2$ |
| 63     | Europium     | Eu | $4d^{10}$                | $4f^7$    | $5s^2$ | $5p^6$ | --   | $6s^2$ |
| 64     | Gadolinium   | Gd | $4d^{10}$                | $4f^7$    | $5s^2$ | $5p^6$ | $5d$ | $6s^2$ |
| 65     | Terbium      | Tb | $4d^{10}$                | $4f^9$    | $5s^2$ | $5p^6$ | --   | $6s^2$ |
| 66     | Dysprosium   | Dy | $4d^{10}$                | $4f^{10}$ | $5s^2$ | $5p^6$ | --   | $6s^2$ |
| 67     | Holmium      | Ho | $4d^{10}$                | $4f^{11}$ | $5s^2$ | $5p^6$ | --   | $6s^2$ |
| 68     | Erbium       | Er | $4d^{10}$                | $4f^{12}$ | $5s^2$ | $5p^6$ | --   | $6s^2$ |
| 69     | Thulium      | Tm | $4d^{10}$                | $4f^{13}$ | $5s^2$ | $5p^6$ | --   | $6s^2$ |
| 70     | Ytterbium    | Yb | $4d^{10}$                | $4f^{14}$ | $5s^2$ | $5p^6$ | --   | $6s^2$ |
| 71     | Lutetium     | Lu | $4d^{10}$                | $4f^{14}$ | $5s^2$ | $5p^6$ | $5d$ | $6s^2$ |

Trivalent neodymium ( $\text{Nd}^{3+}$ ) is the most successful type of active ion for solid-state lasers and thus far has been made to lase in more types of crystal and glass hosts than any other ion. It can operate as either a pulsed or continuous-wave laser with a sharp emission line. The most common emission wavelength is near  $1\mu\text{m}$ , but there are several possible laser transitions in the near-infrared spectral region, and in addition a near-ultraviolet laser line. The two host materials most commonly used for this laser ion are yttrium aluminium garnet (YAG) and glass. When doped in YAG, the Nd: YAG crystal produces laser output primarily at  $1.064\mu\text{m}$ ; when doped in glass, the Nd: glass medium lases at wavelengths ranging from  $1.054$  to  $1.056\mu\text{m}$ , depending upon the type of glass used. Nd ions in YAG crystals are limited to a maximum concentration of 1.0 - 1.5 % [1]. Higher concentration leads to increased collision decay, resulting in a reduced upper laser level lifetime. At room temperature the  $1.064\mu\text{m}$  radiative transition is homogeneous broadened with a narrow emission line width of  $0.45\text{nm}$  and the upper level lifetime is  $230\mu\text{s}$ . Nd:YAG rods have good heat conduction properties, which make them desirable for high-repetition rate laser operation. These have a disadvantage, however, in that they are limited by crystal growth capabilities to small laser rods, of the order of up to  $1\text{cm}$  in diameter and lengths of the order of  $10\text{cm}$ . doping YAG with neodymium results in a blue to violet crystal. Because the material becomes strained at atomic percentages greater than approximately 1.5%, the majority of Nd:YAG crystals are doped at approximately 1%. It is generally accepted that higher doped material (1 to 1.4 %) is better for Q-switched laser performance (due to the higher energy storage) while lower doped material (0.5 to 0.8%) is better to cw (steady-state) laser performance where optical beam quality is important [6].

Nd can be doped to very high concentration in glass. Many types of phosphates and silicate glasses have been used for the lasers. The outstanding practical advantage compared to crystalline materials is the tremendous size capability for high-energy applications. For Nd: glass laser gain media, very large-size laser materials have been produced. It can be fabricated into special laser configurations such as slabs and fibers as well as standard rod designs. Rods of up to  $2\text{m}$  long and  $0.75\text{m}$  in diameter and disks of up to  $0.05\text{m}$  thick have been successfully

demonstrated. The optical quality can be excellent, and beam angles approaching the diffraction limit can be achieved. Glass, of course, is easily fabricated and takes a good optical finish. The fluorescent lifetime is approximately  $300\mu\text{s}$ , and, the emission line width is  $18\text{-}28\text{nm}$ . This is wider than for Nd:YAG by factor of 40 to 60. This increased emission line width (inhomogeneous broadening) in effect reduces the laser gain. The drawback of Nd: glass laser materials is their relatively poor thermal conductivity, which restricts these lasers to relatively low pulse repetition rates for pulsed lasers and a lower operating power for cw lasers [2,3,7]. Therefore, the laser thresholds for glass lasers have been found to run higher than their crystalline counterparts. This leads to thermally induced birefringence and optical distortion in glass laser rods when they are operated at high average powers. Therefore crystalline laser hosts generally offer as advantages over glasses their higher thermal conductivity, narrower fluorescence linewidth, and, in some cases, greater hardness. However, the optical quality and doping homogeneity of crystalline hosts are often poorer, and the absorption lines are generally narrower. A summary of the host crystals used for laser systems is given in Table 2 [8,9,10].

## 2. Nd:YAG Crystal

The Nd:YAG laser is the most commonly used type of solid-state laser at the present time, perhaps surpassing in number the ruby laser. Nd:YAG (Neodymium-doped yttrium aluminium garnet  $\text{Y}_3\text{Al}_5\text{O}_{12}:\text{Nd}^{3+}$ ) is clear (colourless), optically isotropic, of good optical quality, hard  $43\text{m}$  material, whose most familiar application is as a diamond replacement in jewelry. YAG is optically isotropic crystal, of good optical quality, and has a high thermal conductivity ( $0.14\text{ W/cm-K}$ ). YAG is also nonhygroscopic, melts at  $1970^\circ\text{C}$ , and has a Knoop hardness of 1215 (around 8.2 on the Moh's hardness scale), which makes it one of the most durable of the common laser crystals [3,7]. It possesses a cubic structure characteristic of garnets with space group  $\text{Ia}3d$ . The cubic structure of YAG favours a narrow fluorescent linewidth, which results in high gain and low threshold for laser operation. The YAG structure is stable from the lower

temperatures up to the melting point, and no transformations have been reported in the solid phase. The strength and hardness of YAG are lower than ruby but still hard enough so that normal fabrication procedures do not produce any serious breakage problems [1,4]. In the garnet crystal structure the yttrium ion is surrounded by eight oxygen ions in the shape of a distorted cube. In Nd:YAG about 1% of  $Y^{3+}$  is substituted by  $Nd^{3+}$ . The radii of the two rare earth ions differ by about 3%. The larger size of the  $Nd^{3+}$  ion results in polyhedra with sides that are greater in length than those of the  $Al^{3+}$  polyhedra. This distorts the lattice and thus limits the maximum doping concentration to several atomic weight percent. Therefore, with the addition of large amounts of neodymium, strained

crystals are obtained indicating that either the solubility limit of neodymium is exceeded or that the lattice of YAG is seriously distorted by the inclusion of neodymium. Doping introduces a lattice strains and distorts the properties of the optical spectra. The local site symmetry is  $D_2$ . Since the Nd:YAG crystal has good optical quality and high thermal conductivity, making it possible to provide pulsed laser output at repetition rates of up to 100Hz. Nd glass laser is restricted to the repetition rates less than 5Hz by the limitation of the laser material above that repetition rate, however, the performance plummets and the second and most widely used solid-state-laser system.

**Table 2. Laser Host Materials**

| Host             | Symmetry           | Lattice Constants (Å)            | Melting Point ( $^{\circ}C$ ) | Refractive Index (n) | Hardness (Moh) | Thermal Conductivity at room temp (cal/cm $^{\circ}C$ ) | Thermal Expansion Coefficients ( $10^{-6}$ ) |
|------------------|--------------------|----------------------------------|-------------------------------|----------------------|----------------|---------------------------------------------------------|----------------------------------------------|
| $Al_2O_3$        | $D_{3d}$<br>R3C    | 5.12                             | 2040                          | 1.765                | 9              | 0.11                                                    | 5.8                                          |
| $CaF_2$          | $O_h$<br>Fm3m      | 5.451                            | 1360                          | 1.4335               | 4              |                                                         | 19.5                                         |
| $SrF_2$          | $O_h$<br>Fm3m      | 5.78                             | 1400                          | 1.438                |                |                                                         |                                              |
| $BaF_2$          | $O_h$<br>Fm3m      | 6.19                             | 1280                          | 1.475                |                |                                                         |                                              |
| $SrCl_2$         | $O_h$<br>Fm3m      | 7.00                             | 873                           | 1.6                  |                |                                                         |                                              |
| $LaF_3$          | $D_{6h}$<br>C6/mcm | $a_0 = 4.148$<br>$c_0 = 7.354$   | 1493                          |                      |                |                                                         |                                              |
| $CeF_3$          | $D_{6h}$<br>C6/mcm | $a_0 = 4.115$<br>$c_0 = 7.288$   | 1324                          |                      |                |                                                         |                                              |
| $CaWO_4$         | $C_{4h}$<br>I4/a   | 5.24<br>11.38                    | 1570                          | 1.918<br>1.934       | 4.5            |                                                         |                                              |
| $SrWO_4$         | $C_{4h}$<br>I4/a   |                                  | 1566                          |                      |                |                                                         |                                              |
| $CaMoO_4$        | $C_{4h}$<br>I4/a   | 5.23<br>11.44                    | 1430                          | 1.967<br>1.978       | 6              | 0.0095                                                  | 25.5 c axis<br>19.4 a axis                   |
| $PbMoO_4$        | $C_{4h}$<br>I4/a   | 5.41<br>11.08                    | 1070                          |                      |                |                                                         |                                              |
| $Y_2O_3$         | $T_h$<br>Ia3       | 10.6                             | 2450                          |                      |                |                                                         |                                              |
| $Cd_2O_3$        | $T_h$<br>Ia3       | 10.79                            | 2330                          |                      |                |                                                         |                                              |
| $Er_2O_3$        | $T_h$<br>Ia3       | 10.54                            |                               |                      |                |                                                         |                                              |
| $Y_3Al_5O_{12}$  | $O_h$<br>I $_h$ 3d | 12.00                            | 1970                          | 1.83                 | 8.5            | 0.030                                                   | 9.3                                          |
| $Y_3Ga_5O_{12}$  | $O_h$<br>I $_h$ 3d | 12.27                            |                               | 1.93                 | 7.5            |                                                         |                                              |
| $Gd_3Ga_5O_{12}$ | $O_h$<br>I $_h$ 3d |                                  | 1825                          |                      |                |                                                         |                                              |
| $MgF_2$          | $D_{4h}$<br>P4/mmm | $a_0 = 4.6213$<br>$c_0 = 3.0529$ | 1255                          | 1.38                 |                |                                                         |                                              |
| $MgF_2$          | $D_{4h}$<br>P4/mmm | $a_0 = 4.715$<br>$c_0 = 3.131$   | 872                           |                      |                |                                                         |                                              |
| $Ca(NbO_3)_2$    |                    |                                  | 1560                          | 2.07-2.20            |                |                                                         |                                              |

The Nd laser incorporates a four-level system and consequently has a much lower pumping threshold than that of the ruby and other lasers. The upper laser lifetime is relatively long (2.30 $\mu s$  for Nd: YAG and 320 $\mu s$  for Nd: glass) so population can be accumulated over a relatively long duration during the pumping cycle when the laser is used either in the Q-switching mode or as an amplifier. The emission and gain linewidths are 0.45nm for YAG and 28nm for glass. The Nd:YAG crystal produces laser output primarily at 1.064  $\mu m$ . At room temperature, this 1.064 $\mu m$  radiative transition is homogeneously broadened with a narrow emission linewidth of  $1.2 \times 10^{11}$  Hz ( $\Delta\lambda =$

0.45nm) and the upper level lifetime is 230 $\mu s$ . Nd: YAG rods have good heat conduction properties, which make them desirable for high-repetition rate laser operation. They have a disadvantage, however, in that they are limited by crystal growth capabilities to small laser rods, of the order of up to 1cm in diameter and lengths of the order of 10cm. thereby limiting the power and energy output capabilities of this laser. The optical quality of such rods is normally quite good and comparable to the best quality of Czochralski ruby or optical glass [4]. Commercially available laser crystals are grown exclusively by the Czochralski method. Growth rates, dopants, annealing procedures, and final size generally

determine the manufacturing rate of each crystal. The boule axis or growth direction is customarily in the  $\langle 111 \rangle$  direction. The high manufacturing costs of Nd:YAG are mainly caused by the very slow growth rate of Nd:YAG, which is of the order of 0.5mm/hr. Typical boules of 10 to 15cm in length require a growth run of several weeks. In specifying Nd:YAG rods, the emphasis is on size, dimensional tolerance, doping level, and passive optical tests of rod quality. Cylindrical rods with flat ends are typically finished to the following specifications: end flat to  $\lambda/10$ , ends parallel to  $\pm 4$  arc seconds, perpendicularity to rod axis to  $\pm 5$  minutes, rod axis parallel to within  $+ 5^0$  to  $\langle 111 \rangle$  direction. Dimensional tolerances typically are  $\pm 0.5$  mm on length and  $\pm 0.025$ mm on diameter.

**Table 3. Material Properties of Nd: YAG**

|                                                                                       |                                                           |
|---------------------------------------------------------------------------------------|-----------------------------------------------------------|
| Chemical formula                                                                      | Nd: Y <sub>3</sub> Al <sub>5</sub> O <sub>12</sub>        |
| Crystal structure                                                                     | Cubic / garnet                                            |
| Lattice constant                                                                      | 12.01 Å                                                   |
| Weight % Nd                                                                           | 0.725                                                     |
| Atomic % Nd                                                                           | 1.0                                                       |
| Nd atoms/ cm <sup>3</sup>                                                             | $1.38 \times 10^{20}$                                     |
| Melting point                                                                         | 1970 °C                                                   |
| Knoop hardness                                                                        | 1350 +/- 35 kg/mm <sup>2</sup>                            |
| Density                                                                               | 4.56 g/cm <sup>3</sup>                                    |
| Rupture stress                                                                        | $1.3 - 2.6 \times 10^3$ kg/cm <sup>2</sup>                |
| Modulus of elasticity                                                                 | $3 \times 10^3$ kg/cm <sup>2</sup>                        |
| Poisson's ratio                                                                       | 0.28                                                      |
| Thermal expansion coefficient                                                         |                                                           |
| <100> orientation                                                                     | $8.2 \times 10^{-6}$ C <sup>-1</sup> , 0-250 C            |
| <110> orientation                                                                     | $7.7 \times 10^{-6}$ C <sup>-1</sup> , 10-250 C           |
| <111> orientation                                                                     | $7.8 \times 10^{-6}$ C <sup>-1</sup> , 0-250 C            |
| Linewidth                                                                             | 4.5 Å <sup>0</sup>                                        |
| Primary Diode pump Band                                                               | 808.6 nm                                                  |
| Stimulated emission cross section                                                     | $\sigma_{21} = 2.7 - 8.8 \times 10^{-19}$ cm <sup>2</sup> |
| Relaxation time ( <sup>4</sup> I <sub>11/2</sub> → <sup>4</sup> I <sub>9/2</sub> )    | 30 ns                                                     |
| Radiative lifetime ( <sup>4</sup> F <sub>3/2</sub> → <sup>4</sup> I <sub>11/2</sub> ) | 550 μs                                                    |
| Spontaneous fluorescence lifetime                                                     | 230 μs                                                    |
| Photon energy at 1.06 μm                                                              | $h\nu = 1.86 \times 10^{-19}$ J                           |
| Index of refraction                                                                   | 1.82 (at 1.064 μm)                                        |
| Nonlinear index                                                                       | $3 \times 10^{-13}$ esu                                   |
| Scatter losses                                                                        | $\alpha_{sc} \approx 0.002$ cm <sup>-1</sup>              |

**Table 4. Thermal properties of Nd: YAG**

| Property                | Units                             | 300K                 | 200K | 100K |
|-------------------------|-----------------------------------|----------------------|------|------|
| Thermal conductivity    | Wcm <sup>-1</sup> K <sup>-1</sup> | 0.13                 | 0.21 | 0.58 |
| Specific heat           | Wsg <sup>-1</sup> K <sup>-1</sup> | 0.59                 | 0.43 | 0.13 |
| Thermal diffusivity     | Cm <sup>2</sup> s <sup>-1</sup>   | 0.046                | 0.10 | 0.92 |
| Thermal expansion       | K <sup>-1</sup>                   | 7.5                  | 5.80 | 4.25 |
| $\partial n/\partial T$ | K <sup>-1</sup>                   | $7.3 \times 10^{-6}$ | -    | -    |

**Table 5. Index of refraction and reflectance of Nd:YAG**

| Wavelength (nm) | <i>n</i> | <i>R</i> |
|-----------------|----------|----------|
| 266             | 1.9278   | 0.1004   |
| 354             | 1.8725   | 0.0923   |
| 532             | 1.8368   | 0.0870   |
| 808             | 1.8217   | 0.0848   |
| 946             | 1.8186   | 0.0843   |
| 1030            | 1.8173   | 0.0842   |
| 1064            | 1.8169   | 0.0841   |
| 1333            | 1.8146   | 0.0838   |
| 1444            | 1.8140   | 0.0837   |
| 1500            | 1.8137   | 0.0836   |
| 1640            | 1.8132   | 0.0836   |
| 2014            | 1.8123   | 0.0834   |
| 2097            | 1.8121   | 0.0834   |
| 2123            | 1.8121   | 0.0834   |
| 2940            | 1.8113   | 0.0833   |

An energy-level diagram for Nd<sup>3+</sup> doped in a YAG host material is shown in Figure 1 (a). The relevant laser levels are slightly lowered for doping in glass as compared to YAG, as shown in below Figure 1 (b). The upper laser level is shifted downward by 112cm<sup>-1</sup> and the lower laser level is shifted downward by 161cm<sup>-1</sup>, producing a net decrease in the laser wavelength for glass. The excitation bands occur in the blue and the green. The pump energy then transfers nonradiatively (collisionally) to the upper laser level <sup>4</sup>F<sub>3/2</sub>. The laser terminates on the <sup>4</sup>I<sub>11/2</sub> lower level, from which collisional decay takes the population back to the ground state. Two other radiative transitions in the Nd ion are also used as laser transitions. They originate from the same upper laser level as the 1.064 μm transition and decay to the <sup>4</sup>I<sub>13/2</sub> level radiating at 1.35 μm and to the <sup>4</sup>I<sub>9/2</sub> level producing 0.88-μm radiation. These transitions have lower gain than the 1.064 μm transition and therefore are not as easily made to lase [12,13,14].

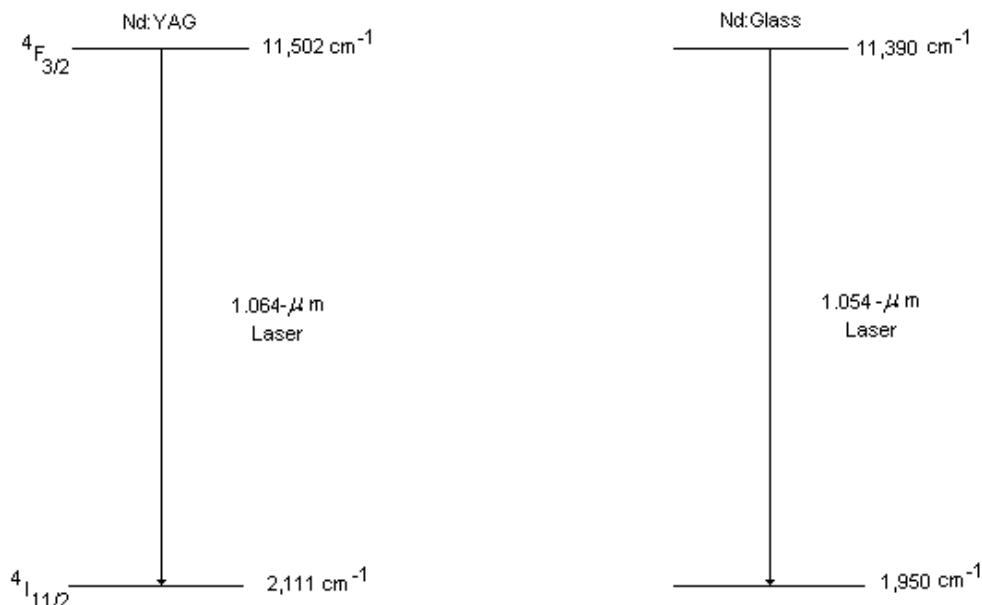
**Figure 1.** Comparison of energy levels of the laser transition for Nd doped in YAG and glass

Table 6. Typical Nd: YAG and Nd: Glass Laser Parameters

| Laser parameters                                                        | Nd:YAG                                                                         | Nd: Glass                                                           |
|-------------------------------------------------------------------------|--------------------------------------------------------------------------------|---------------------------------------------------------------------|
| Laser Wavelength ( $\lambda$ )                                          | 1.064 $\mu\text{m}$                                                            | 1.054-1.062 $\mu\text{m}$                                           |
| Laser Transition Probability ( $A$ )                                    | $4.3 \times 10^7/\text{s}$                                                     | 2.9 to $3.4 \times 10^7/\text{s}$                                   |
| Upper Laser Level Lifetime ( $\tau$ )                                   | 230 $\mu\text{s}$                                                              | 290 – 340 $\mu\text{s}$                                             |
| Stimulated Emission Cross Section ( $\sigma$ )                          | $6.5 \times 10^{-23} \text{m}^2$                                               | 2.9 to $4.3 \times 10^{-24} \text{m}^2$                             |
| Spontaneous Emission Linewidth and Gain Bandwidth, FWHM ( $\Delta\nu$ ) | $1.2 \times 10^{11}/\text{s}$<br>( $\Delta\lambda = 0.45 \text{nm}$ )          | $7.5 \times 10^{11}/\text{s}$<br>( $\Delta\lambda = 28 \text{nm}$ ) |
| Inversion Density ( $\Delta N$ )                                        | $1.6 \times 10^{25}/\text{m}^3$                                                | $8 \times 10^{25}/\text{m}^3$                                       |
| Small Signal Gain Coefficient ( $g$ )                                   | 10/m                                                                           | 3/m                                                                 |
| Laser Gain-Medium Length ( $L$ )                                        | 0.1-0.15 m                                                                     | 0.1 m                                                               |
| Single-Pass Gain ( $e^{g\Delta L}$ )                                    | 2 - 20                                                                         | 1.3                                                                 |
| Doping Density                                                          | $1.4 \times 10^{26}/\text{m}^3$                                                | $4.6 \times 10^{26}/\text{m}^3$                                     |
| Index of Refraction of Gain Medium                                      | 1.82                                                                           | 1.50 – 1.57                                                         |
| Operating Temperature                                                   | 300 K                                                                          | 300 K                                                               |
| Thermal Conductivity of Laser Rod                                       | 13 W/m-K                                                                       | $\approx 1 \text{ W/m-K}$                                           |
| Thermal Expansion Coefficient of Laser Rod                              | $6.9 \times 10^{-6}/\text{K}$                                                  | $8.5 \text{ to } 14 \times 10^{-6}/\text{K}$                        |
| Pumping Method                                                          | Optical (flash lamp or Laser)                                                  |                                                                     |
| Pumping Bands                                                           | 300 – 900 nm, with strongest peaks at 810 nm and 750 nm (peaks wider in glass) |                                                                     |
| Output Power                                                            | 1 J/pulse                                                                      | Up to 10 kJ/pulse in large amplifiers                               |
| Mode                                                                    | Single-mode or multi-mode                                                      |                                                                     |

## 2.1. Energy Levels of $\text{Nd}^{3+}$

The electronic configuration for the 60 electrons of a neodymium atom is:

$1s^2 2s^2 2p^6 3s^2 3p^6 3d^{10} 4s^2 4p^6 4d^{10} 4f^4 5s^2 5p^6 5d^0 6s^2$ . The first nine sets of orbitals make up the filled core, while the optically active electrons are in the partially filled 4f orbitals. The latter are shielded by the electrons in the outermost 5s through 6s orbitals. The trivalent neodymium ion has given up three electrons, two from the outer 6s orbitals and one from the 4f orbitals, leaving a configuration of Xe ( $4f^3 5s^2 5p^6$ ). The three 4f electrons are the ones that play the dominant role in determining the optical properties of the ion. Although the transitions giving rise to the optical spectra take place between different levels of the  $4f^3$  configuration, it is also important to know the positions of the energy levels of the  $4f^{N-1}5d$  configurations since configuration interaction is critical in determining spectral line strengths. The Russell-Saunders coupling approach can be used to determine the electronic terms of the free ion with three electrons, each having quantum numbers  $n = 4$  and  $l = 3$ . Due to the shielding of the outer-shell electrons, the crystal-field splitting is always treated in the weak-field limits, so spin-orbit coupling is applied first to determine free-ion multiplets. The types of spectroscopic terms available for  $\text{Nd}^{3+}$  ions can be determined by using appropriate combinations of single-electron orbitals and applying the Pauli's exclusion principle. Since all of the optically active electrons have same values of  $n$  and  $l$ , there are only certain combinations of the quantum numbers  $m_l$  and  $m_s$  that are allowed. Since  $l = 3$  for each of the electrons, the largest value of the total angular momentum quantum number could be 9 so  $M_L$  should run from 0 to  $\pm 9$  in integer steps. However, the only way for the orbitals angular momenta of the three electrons to couple to give  $L = 9$  would result in two of the electrons having an identical set of quantum numbers, which is not allowed. The spin angular momenta of the three electrons can couple to give quartets or doublets, so  $M_S = \pm 3/2, \pm 1/2$ . A table of single-electron states that contribute to the multielectron terms can be constructed and the results are shown in Table 7. Only the positive  $M_L$  - positive  $M_S$  quarter of the table is shown since the table is symmetric and thus all of the required information can be obtained from this quarter. Here the single-electron

states are represented by ( $m_{l1}^{\pm}, m_{l2}^{\pm}, m_{l3}^{\pm}$ ) where the + or - superscript designates spin up or spin down, respectively. These are placed in the  $M_L$  row and  $M_S$  column of an appropriate term. Since the largest values of  $M_L$  and  $M_S$  equal  $L$  and  $S$ , respectively, for a given term, Table 7 can be used to determine the spectroscopic terms of a  $4f^3$  ion. The highest  $M_L$  row in the table has single-electron states occupying only the cells in the  $M_S = \pm 1/2$  columns. Since this cell represents  $M_L = 8$ , these must belong to a  ${}^2L$  term. One of the single-electron states occupying only the cells in the  $M_S = \pm 1/2$  columns will also belong to this term thus can be eliminated. This leaves the highest occupied cells those with  $M_L = L = 7$  and  $M_S = \pm 3/2$ . The states in these cells belong to a  ${}^4I$  term with additional states in all the remaining cells. This procedure can be followed until all of the single-electron states have been associated with multielectron terms resulting in the identification of 17 terms:  ${}^2L, {}^2K, {}^4I, {}^2I, {}^2H, {}^2H, {}^4G, {}^2G, {}^2G, {}^4F, {}^2F, {}^2F, {}^4D, {}^2D, {}^2D, {}^2P, {}^4S$ . Next these terms must be placed in order to ascending energy. Using Hund's rule, implies that the  ${}^4I$  term is the ground state, and the energies of the other terms with respect to the ground state must be determined. As with transition-metal ions, perturbation theory is used to determine the energy levels with the zero-order perturbation being the electrons in the 4f orbital moving independently of each other in the central field of the nucleus and the inner-shell electrons. Under these conditions, all energy levels of a given  $4f^3$  configuration are degenerate. The Coulomb interaction between the optically active electrons is treated as one perturbation and the spin-orbit interaction of the electrons is treated as another perturbation. This gives a good approximation for calculating the energy levels. However, for rare-earth ions the interactions between electrons in different configurations can also be important in some cases.

The spin-orbit interaction is the same order of magnitude as the Coulomb interaction for the rare-earth ions and therefore must be treated before treating the crystal-field perturbation. The qualitative splitting of the terms into multiplets follows the description of angular momentum coupling. The values of the  $J$  quantum numbers for the multiplets of a term with quantum numbers  $L$  and  $S$  run in integer steps from  $L - S$  to  $L + S$ . Thus the ground term of  $\text{Nd}^{3+}$  has the four multiplets  ${}^4I_{9/2}, {}^4I_{11/2}, {}^4I_{13/2}$ , and  ${}^4I_{15/2}$  with the first of these being lowest in

energy because the electronic configuration of this ion is less than a half-field shell. The four multiplets of the

metastable state range from  ${}^4F_{3/2}$  to  ${}^4I_{9/2}$ . Some of these splitting is shown in Figure 2 [15,16].

**Table 7. Single-electron states for a  $4f^3$ -electron configuration**

| L | S=1/2                                                                                                  | S=3/2                                                                 | Term           |
|---|--------------------------------------------------------------------------------------------------------|-----------------------------------------------------------------------|----------------|
| L | $(3^3 2^2)$                                                                                            |                                                                       | ${}^2L$        |
| K | $(3^3 1^+)(3^2 2^+)$                                                                                   |                                                                       | ${}^2K$        |
| I | $(3^3 0^+)(3^2 1^+)$                                                                                   | $(3^2 1^+)$                                                           | ${}^4I, {}^2I$ |
| H | $(3^3 -1^+)3(3^2 0^+)(3^+ 1^+)(2^2 1^+)$                                                               | $(3^2 0^+)$                                                           | $2^2H$         |
| G | $(3^3 -2^+)3(3^2 -1^+)3(3^+ 0^+)(2^2 0^+)(2^+ 1^+)$                                                    | $(3^+ 0^+)(3^2 -1^+)$                                                 | ${}^4G, 2^2G$  |
| F | $(3^3 -3^+)3(3^2 -2^+)3(3^+ -1^+)(3^0 0^+)(3^+ 1^+)(2^2 -1^+)$                                         | $(3^2 -2^+)(3^+ -1^+)(0^2 1^+)$                                       | ${}^4F, 2^2F$  |
| D | $3(3^2 -3^+)3(3^+ -2^+)3(3^0 -1^+)(2^+ 0^+)(3^2 -2^+)(1^+ 0^+)$                                        | $(3^2 -3^+)(3^+ -2^+)(0^+ 3^+ -1^+)(2^+ 1^+ -1^+)$                    | ${}^4D, 2^2D$  |
| P | $3(3^+ 1^+ -3^+)3(3^0 -2^+)(3^+ -1^+)(2^2 -3^+)(2^+ 1^+ -2^+)(2^+ 0^+ -1^+)(1^+ 1^+ -1^+)(1^+ 0^+)$    | $(3^+ 1^+ -3^+)(3^+ -2^+ 0^+)(0^+ 2^+ -1^+)(2^+ 1^+ -2^+)$            | ${}^4P$        |
| S | $3(3^0 -3^+)3(-3^+ 1^+ 2^+)3(2^+ 0^+ -2^+)(2^+ -1^+ -1^+)(3^+ -1^+ -2^+)3(1^+ 0^+ -1^+)(1^+ 1^+ -2^+)$ | $(3^0 -3^+)(2^+ -3^+ 1^+)(0^+ 2^+ -2^+)(0^+ 1^+ -1^+)(-2^+ 3^+ -1^+)$ | ${}^4S$        |

### 2.2. Laser Transitions in Nd: YAG

The Nd:YAG laser is a four-level system as depicted by a simplified energy level diagram in and Figure 2. The 1.064 and 1.061- $\mu\text{m}$  transitions, provide the lowest threshold laser lines in Nd:YAG. The main laser transition occurs at 1064nm due to the  ${}^4F_{3/2} - {}^4I_{11/2}$  transition, originates from the  $R_2$  component of the  ${}^4F_{3/2}$  level and terminates at the  $Y_3$  component of the  ${}^4I_{11/2}$  level. The width of the laser transition is 4.5  $\text{Å}$  and the stimulated emission cross section is  $6.5 \times 10^{-19} \text{cm}^2$ . The index of refraction at the wavelength of the laser transition is 1.82, and the scattering loss coefficient for a typical laser crystal is  $0.002 \text{cm}^{-1}$ . At room temperature only 40% of the  ${}^4F_{3/2}$  population is at level  $R_2$ ; the remaining 60% are at the lower sublevel  $R_1$  according to Boltzmann's law, i.e. at room temperature the 1.064 $\mu\text{m}$  line  $R_2 \rightarrow Y_3$  is dominated, while at low temperatures the 1.061  $\mu\text{m}$   $R_1 \rightarrow Y_1$  has the lower threshold [17]. If the laser crystal is cooled, additional laser transitions are obtained, mostly the 1.839  $\mu\text{m}$  line and the 0.946  $\mu\text{m}$  line. Lasing takes place only by  $R_2$  ions whereby the  $R_2$  level population is replenished from  $R_1$  by thermal transitions. The ground level of Nd:YAG is the  ${}^4I_{9/2}$  level. There are a number of relatively broad energy levels, which together may be viewed as comprising pump level 3. Of the main pump bands shown, the 0.81 $\mu\text{m}$  and 0.75 $\mu\text{m}$  bands are the strongest. The terminal laser level is 2111  $\text{cm}^{-1}$  above the ground state and thus the population is a factor of  $\exp(\Delta E/kT) \approx \exp(-10)$  of the ground state density. Since the terminal level is not populated thermally, the threshold condition is easy to obtain.

The upper laser level,  ${}^4F_{3/2}$ , has a fluorescent efficiency greater than 99.5% [12] and a radiative lifetime of 230  $\mu\text{s}$ . The branching ratio of emission from  ${}^4F_{3/2}$  is as follows [18]:  ${}^4F_{3/2} \rightarrow {}^4I_{9/2} = 0.25$ ,  ${}^4F_{3/2} \rightarrow {}^4I_{11/2} = 0.60$ ,  ${}^4F_{3/2} \rightarrow {}^4I_{13/2} = 0.14$ , and  ${}^4F_{3/2} \rightarrow {}^4I_{15/2} < 0.01$ . This means that almost all the ions transferred from the ground level to the pump bands end up at the upper laser level, and 60% of the ions at the upper laser level cause fluorescent output at the  ${}^4I_{11/2}$  manifold. Figure-3 shows the absorption spectrum for the Nd-ions in YAG. Under normal operating conditions the Nd:YAG laser oscillates at room temperature on the strongest  ${}^4F_{3/2} \rightarrow {}^4I_{11/2}$  transition at 1.064  $\mu\text{m}$ , which is homogeneously broadened by thermally activated lattice vibrations. The values of stimulated emission cross-section for the extensively measured 1.06- $\mu\text{m}$  line ranges from 2.7 to 8.8  $10^{-19} \text{cm}^2$  [11,18]. It is possible, however, to obtain oscillation at other wavelengths by inserting a

dispersive prism in the resonator, by utilizing a specially designed resonator reflector as an output mirror [19], or by employing highly selective dielectrically coated mirrors [20]. These elements suppress laser oscillation at the undesirable wavelength and provide optimum conditions at the wavelengths desired. With this technique over 20 transitions have been made to lase in Nd:YAG. The effective cross section at room temperature of the important transitions and the measured relative thresholds of those transitions at which room-temperature cw oscillation have been observed are given in Table 8 [4]. There is a second prominent laser transition for Nd:YAG that originates on the same metastable state but terminates on the  ${}^4I_{13/2}$  level. This occurs at 1.338 $\mu\text{m}$  and has a cross section that is about four times smaller than that of the main laser line [21]. The slope efficiency of this laser transition is somewhat less than that of the main laser line which is consistent with the lower energy of the photons involved in the transition. The threshold for lasing is higher; the gain lower, and the maximum output power is lower for the 1.338- $\mu\text{m}$  emission as compared to 1.034- $\mu\text{m}$  emission. Both lasing transitions can be operated in cw, pulsed, and Q-switched operation, the 1.064- $\mu\text{m}$  line typically provides pulses with temporal widths between about 12 and 75 ns while the 1.338- $\mu\text{m}$  line typically provides pulses between about 100 and 400 ns [23,24,25,26].

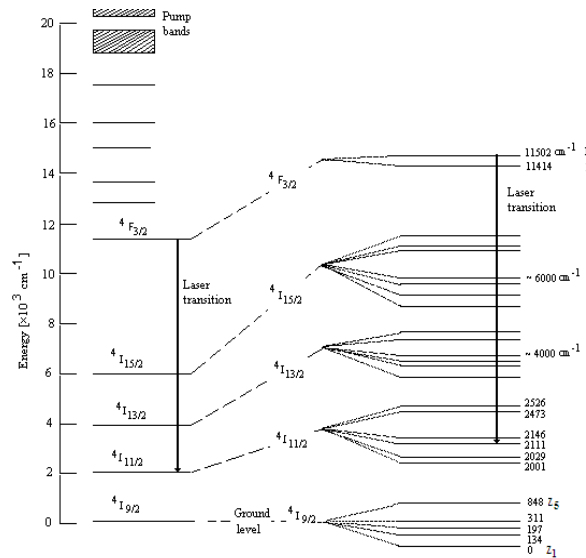


**Figure 2. Energy level diagram of Nd: YAG**

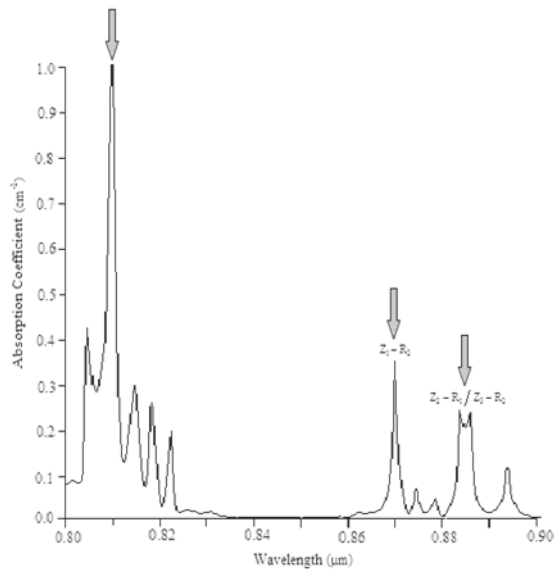


Figure 3. Absorption Spectrum of Nd:YAG

Table 8. Main transitions in Nd:YAG

| Transitions Levels                 | Wavelength [μm] | Peak effective room temperature cross section $\sigma$ [ $10^{-19} \text{ cm}^2$ ] | Measured relative room temperature cw laser threshold |
|------------------------------------|-----------------|------------------------------------------------------------------------------------|-------------------------------------------------------|
| $^4F_{3/2} \rightarrow ^4I_{9/2}$  | 0.939           | 0.81                                                                               |                                                       |
|                                    | 0.946           | 1.34                                                                               |                                                       |
|                                    | 1.0520          | 3.10                                                                               | 2.08                                                  |
|                                    | 1.0551          | 0.20                                                                               |                                                       |
|                                    | 1.0615          | 6.65                                                                               | 1.15                                                  |
|                                    | 1.0641          | 8.80                                                                               | 1.00                                                  |
|                                    | 1.0682          | 1.10                                                                               |                                                       |
|                                    | 1.0738          | 4.00                                                                               | 1.22                                                  |
|                                    | 1.0779          | 1.55                                                                               |                                                       |
|                                    | 1.1055          | 0.32                                                                               |                                                       |
| $^4F_{3/2} \rightarrow ^4I_{11/2}$ | 1.1122          | 0.79                                                                               | 2.17                                                  |
|                                    | 1.1161          | 0.77                                                                               | 2.26                                                  |
|                                    | 1.1225          | 0.72                                                                               | 2.36                                                  |
|                                    | 1.3190          | 1.50                                                                               | 1.60                                                  |
|                                    | 1.3350          | 0.92                                                                               |                                                       |
|                                    | 1.3380          | 1.50                                                                               | 2.17                                                  |
|                                    | 1.3420          | 0.63                                                                               |                                                       |
|                                    | 1.3530          | 0.35                                                                               |                                                       |
|                                    | 1.3570          | 0.88                                                                               |                                                       |

## Conclusion

Trivalent neodymium ( $\text{Nd}^{3+}$ ) is the most successful type of active ion for solid-state lasers and thus far has been made to lase in more types of crystal and glass hosts than any other ion. It can operate as either a pulsed or continuous-wave laser with a sharp emission line. The two host materials most commonly used for this laser ion are yttrium aluminium garnet (YAG) and glass. When doped in YAG, the Nd:YAG crystal produces laser output primarily at  $1.064 \mu\text{m}$ ; when doped in glass, the Nd: glass medium lases at wavelengths ranging from  $1.054$  to  $1.056 \mu\text{m}$ , depending upon the type of glass used. Nd ions in YAG crystals are limited. At room temperature the  $1.064 \mu\text{m}$  radiative transition is homogeneous broadened with a narrow emission line width of  $0.45 \text{ nm}$  and the upper level lifetime is  $230 \mu\text{s}$ . Nd can be doped to very

high concentration in glass. The outstanding practical advantage compared to crystalline materials is the tremendous size capability for high-energy applications. The fluorescent lifetime is approximately  $300 \mu\text{s}$ , and, the emission line width is  $18\text{-}28 \text{ nm}$ .

## References

- [1] K. J. Kuhn; *Laser Engineering*, Prentice Hall Pub., 1998.
- [2] L. R. Marshall, A. D. Hays, H. J. Kasinski, and R. Burnham; "Highly efficient optical parametric oscillators", *SPIE*, 1419: 141-152, 1991.
- [3] R. D. Stultz, D. E. Nieuwsma, E. Gregor; *SPIE*, 1419: 64-74, 1991.
- [4] Walter Koechner, *Solid State Laser Engineering*, 5<sup>th</sup> ed., Springer Berlin, 1999.
- [5] William T. Silfvast, *Laser Fundamentals*, Cambridge University Press, 1991.
- [6] V. J. Corcoran; "High-repetition-rate eyesafe rangefinders" *SPIE*, 1419: 160-163, 1991.
- [7] J. A. Skidmore, M. A. Emanuel, R. J. Beach, B. L. Freitas, N. W. Carlson, C. D. Marshall, W. J. Bennett, R. W. Solaz, D. P. Bour, and D. W. Treat; "New diode wavelengths for pumping solid state lasers", *SPIE Proceedings*, 2382: 106-116, 1997.
- [8] J.E. Geusic, H.M. Marcos, L.G. Van Uitert; "LASER OSCILLATIONS IN Nd - DOPED YTTRIUM ALUMINUM, YTTRIUM GALLIUM AND GADOLINIUM GARNETS", *Appl. Phys.Letters* 4(10): 182, 1964.
- [9] Z. J. Kiss and R. J. Pressley; "Crystalline solid lasers", *Proc. IEEE* 54(10): 1236, 1966.
- [10] Z. J. Kiss and R. J. Pressley; "Crystalline Solid Lasers". *Appl. Opt.*, 5(10): 1474-1486, 1966.
- [11] R. V. Alves, R. A. Buchanan, K. A. Wickersheim, E. A. C. Yates; "Neodymium - Activated Lanthanum Oxysulfide: A New High - Gain Laser Material", *J. Appl. Phys.* 42(8): 3043, 1971.
- [12] T. Kushida, J. E. Geusic; "Optical Refrigeration in Nd-Doped Yttrium Aluminum Garnet", *Phys. Rev. Letters*, 21(16): 1172, 1968.
- [13] W. F. Krupke, M. D. Shinn, J. E. Marion, J. A. Caird, and S. E. Stokowski; "Spectroscopic, optical, and thermomechanical properties of neodymium- and chromium-doped gadolinium scandium gallium garnet", *J. Opt. Soc. Am. B*, 3(1): 102, 1986.
- [14] R. C. Powell, S. A. Payne, L. L. Chase and G. D. Wilke; "Index-of-refraction change in optically pumped solid-state laser materials", *Opt. Lett.*, 14(22): 1204-1206, 1989.
- [15] G.H. Dieke and H.M. Crosswhite; "The Spectra of the Doubly and Triply Ionized Rare Earths", *Appl. Opt.*, 2(7): 675, 1963.
- [16] B. R. Judd; "Optical Absorption Intensities of Rare-Earth Ions", *Phys Rev.*, 127(3): 750, 1962.
- [17] M. Birnbaum; "Stimulated emission cross section at  $1.061 \mu\text{m}$  in Nd:YAG", *J. Appl. Phys.*, 44(6): 2928, 1973.
- [18] T. Kushida, H. M. Marcos, J. E. Geusic; "Laser Transition Cross Section and Fluorescence Branching Ratio for  $\text{Nd}^{3+}$  in Yttrium Aluminum Garnet". *Phys. Rev.*, 167(2): 289-291, 1968.
- [19] H. F. Mahlein; *IEEE J. Quant. Electr.* QE-6: 529, 1970.
- [20] C. G. Bethea; *IEEE J. Quant. Electr.* QE-9: 254, 1973.
- [21] N.P. Barnes, D.J. Gettemy, L. Esterowitz, and R.E. Allen; *IEEE J. Quant. Electr.* QE-23, 1434, 1987.
- [22] F. J. Duarte, *Tunable Laser Optics*, Elsevier-Academic, New York, 2003.
- [23] D. Y. Shen et al., "Highly efficient in-band pumped Er:YAG laser with 60 W of output at  $1645 \text{ nm}$ ", *Opt. Lett.* 31(6): 754-756, 2006.
- [24] Li Chaoyang et al., "106.5 W high beam quality diode-side-pumped Nd:YAG laser at  $1123 \text{ nm}$ ", *Opt. Express* 18(8): 7923-7928, 2010.
- [25] X.Delen et al, "34 W continuous wave Nd:YAG single crystal fiber laser emitting at  $946 \text{ nm}$ ", *Appl. Phys. B* 104(1): 1, 2011.
- [26] H.C. Lee et al, "Diode-pumped continuous-wave eye-safe Nd:YAG laser at  $1415 \text{ nm}$ ", *Opt. Lett.* 37(7): 1160, 2012.